# Evaluation of Plasmonic Optical Heating by Thermal Lens Spectroscopy

Túlio de Pedrosa, Georges Boudebs, Renato de Araujo

# Evaluation of plasmonic optical heating by thermal lens spectroscopy

Túlio de L. Pedrosa[1], Georges Boudebs[2], Renato E. de Araujo[1*]

[1*]Laboratory of Biomedical Optics and Imaging, Federal University of Pernambuco, Rua Acadêmico Hélio Ramos, Recife-PE, 50740-530, Brazil.
[2]Univ. Angers, LPHIA, SFR MATRIX, City, F-49000, Angers, France.

*Corresponding author(s). E-mail(s): renato.earaujo@ufpe.br;
Contributing authors: pedrosatulio@gmail.com;
georges.boudebs@univ-angers.fr;

**Abstract**

This work reveals the rules of using figures-of-merit on selecting efficient plasmonic nanoheaters. Here, a size dependence of plasmonic nanoparticle optical heating was disclosed. The continuous laser heating of gold nanospheres is evaluated exploring a theoretical approach and thermal lens spectroscopy, which allowed identifying micro-degree temperature changes of laser heated colloidal gold nanospheres of varying sizes. Our findings indicate that the temperature of photoheating colloidal particles rises accordingly to the Joule number values. The optimal gold nanospheres diameter for efficient colloidal laser heating was identified to be 50 nm. Moreover, we demonstrated that long-time domain measurements of colloidal sample enable the identification of single particle intermediate steady-state temperature. Considering a single particle, nanospheres with diameter larger than 80 nm exhibit superior heating performance than smaller particles, revealing that the optimal particle size for single particle optical heating applications is different from the optimal particle size for collective heating of nanoparticles. Our results pave the way for the rational use of plasmonic nanoheaters in photothermal applications.

**Keywords:** Gold nanoparticles, Thermoplasmonics, Thermal lens spectroscopy, Localized surface plasmon resonance



This article has been published in Plasmonics, Springer:
Get Citation:
de Pedrosa, T. L., Boudebs, G., & de Araujo, R. E. (2023). "Evaluation of Plasmonic Optical Heating by Thermal Lens Spectroscopy." Plasmonics, 1-6.

Submitted author version.

https://doi.org/10.1007/s11468-023-02120-4

# 1 Introduction

Metallic nanoparticles (NP), when illuminated by a beam of light, are capable of supporting plasmon resonance when excited at the proper wavelength, a product of the damped oscillation of free electrons on the metal nanostructure lattice. Such phenomena can lead to the emergence of remarkable effects, among which plasmon-mediated temperature increase has been the subject of many recent investigations [1–4]. Their applications in life and biomedical sciences have been pursued with a great deal of interest. Photothermal Therapy, for instance, is a technique that may explore nanoheaters to induce localized temperature increase in tissues, enabling cell death mechanisms with applications in cancer treatment [5]. Microbubble formation is another effect that arises due to photoheating. In that case, the plasmonic energy dissipation is responsible for the initial vaporization around the particle, while adsorbed gases lead to nucleation and promote microbubble growth [6]. In this perspective, the formation of microbubbles has been exploited to aid the transport of molecules through cell membranes in optoporation applications [7, 8]. Metallic NPs have also been explored in photoacoustic imaging. The thermoelastic expansion of the medium caused by laser absorption generates a strong photoacoustic signal that enhances image contrast and combines the high resolution achieved by optical imaging techniques with high penetration depth capabilities provided by ultrasound methodologies [9].

Evaluating the performance of nanoparticles as nanoheaters is a fundamental step to the development of efficient platforms and techniques that rely on either distributed or localized heat generation. The assessment of temperature response enables the development and use of high-performance nanoparticles for effective thermal applications. In this sense, temperature increase can be measured by thermocouples [10] and thermal cameras [11, 12]. Such techniques, however, are only capable of assessing the collective heating of the sample, with slow response time. Alternatively, a straightforward strategy to probe nanoheaters using a laser beam to assess temperature change was proposed using thermal lens (TL) measurements [13, 14].

Effective methods for choosing efficient plasmonic particles for photoheating in thermal applications are still scarcely explored. On selecting metallic nanoparticles for photothermal applications, the identification of nanostructures with a high absorption cross-section ($\sigma_{\text{abs}}$) is generally required. Strong light absorption and effective light-to-thermal energy conversion are needed for a rational use of plasmonic nanoheaters. Nanoparticles with high $\sigma_{\text{abs}}$ values have the ability to significantly absorb light, resulting in their temperature rise. The ability of a NP to lose heat to its surroundings is reliant on its surface area. To grant efficient heat loss, the NP surface area must be maximized. Thus, NP morphology becomes relevant to thermoplasmonics applications.

In general, by increasing the size of plasmonic particles, not only the absorption cross-section is enhanced, but the scattering cross-section value also rises. In that case, light energy is strongly scattered to the surrounding medium of the NP. The plasmonic heating induced by pulsed lasers or continuum-wave (CW) sources are governed by distinct dynamics, and therefore, the features of the excitation source should also be considered to identify efficient nanoheaters.

An effective way to quantify the ability of nanoparticles to generate heat under a short pulse illumination is by evaluating the Joule Number (Jo) of the nanostructure, which is given by [15]:

$$J_{\mathrm{o}} = \frac{\lambda_{\mathrm{ref}}}{2\pi} \left( \frac{\sigma_{\mathrm{abs}}}{V_{\mathrm{np}}} \right), \tag{1}$$

where, $V_{\mathrm{np}}$ is the volume of the nanoparticle and $\lambda_{\mathrm{ref}} = 1240$ nm is the reference wavelength of a photon with energy of 1 eV.

The heating of a single metallic nanoparticle under continuous optical excitation is depicted by the Laplace equation, in which the solution can be obtained considering the single particle as a continuous source of energy [16]. The temporal dynamic heating of a nanostructure is generally fast (ps to ns regime), characterized by a thermalization time, $\tau_{\mathrm{np}}$. From the Laplace equation and considering a long illumination time, greater than $\tau_{\mathrm{np}}$, the spatial and temporal dependency of the temperature outside the nanoparticle can be described as [17]:

$$T(r,t) - T_{\infty} = \frac{P_{\mathrm{abs}}}{4\pi\kappa_{\mathrm{m}} r} \left( 1 - \frac{1}{\sqrt{\pi t/\tau_{\mathrm{m}}}} \right), \tag{2}$$

for $r \geqslant a$ and $t \geqslant \tau_{\mathrm{m}}/\pi$, with $\kappa_{\mathrm{m}}$ and $\tau_{\mathrm{m}}$ being respectively the thermal conductivity and the thermalization constant of the medium and $P_{\mathrm{abs}}$ ($= \sigma_{\mathrm{abs}}\mathrm{I}$ ) is the power absorbed by the structure and $T_{\infty}$ is the temperature far away from the nanoparticle, i.e., the initial temperature of the system. Here, $r$ is the distance from the center of the NP and $a$ is the NP radius. Thus, equation 2 describes the system spatial-temporal temperature variation. For $t \gg \tau_{\mathrm{m}}$, the solution of the Laplace equation reaches the steady-state [18], and the maximum temperature of the nanoparticle at the interface ($r = a$) becomes:

$$\Delta T_{\mathrm{np}} = \frac{\sigma_{\mathrm{abs}} I}{4\pi\kappa_{\mathrm{m}} a}, \tag{3}$$

for $I$ the intensity (optical power density) of the laser source. The NP temperature variation is directly proportional to the ratio of its absorption cross-section to the NP radius. Therefore, to evaluate the steady-state temperature of single plasmonic particle under continuous illumination, Pedrosa et al. introduced a new figure of merit, named Steady-State Factor ($\mathrm{S^2F}$), given by [12]:

$$S^2F = \sigma_{\mathrm{abs}}/a. \tag{4}$$

Through theoretical analysis, the Steady-State Factor was initially explored to identify optimal dimensions (length and diameter) of gold nanorods for effective CW infrared photothermal conversion [12].

By illuminating a plasmonic colloidal volume, the global temperature rise ($\Delta T_{\mathrm{global}}$) of the ensemble is proportional to the absorbed light energy. Therefore:

$$\Delta T_{\mathrm{global}} \propto C_{\mathrm{np}} \sigma_{\mathrm{abs}}, \tag{5}$$

where $C_{\mathrm{np}}$ is the concentration of nanoparticles. Considering a colloid of gold nanospheres, with gold mass concentration $C_{\mathrm{m}}$, one can infer that:

$$\Delta T_{\text{global}} \propto \frac{C_{\text{m}}}{\rho_{\text{Au}}} \frac{\sigma_{\text{abs}}}{V_{\text{np}}}, \tag{6}$$

where $\rho_{\text{Au}}$ is the gold mass density. Therefore, by optically heating a plasmonic colloid, the change of the global temperature should be proportional to the nanoparticle Joule Number, i.e. $\Delta T_{\text{global}} \propto \text{J}_{\text{o}}$.

The global temperature increase rises from the collective heat of individual nanoparticles. This superposition effect can be described by [18]:

$$\Delta T_{\text{global}} = \sum_{n=1}^{\#_{\text{np}}} \frac{\sigma_{\text{abs}} I}{4\pi\kappa_{\text{m}}|\vec{r} - \vec{r_n}|}, \tag{7}$$

where $\#_{\text{np}}$ is the number of particles in the illuminated volume.

On the analyzes of the optical heating of a plasmonic colloid, an analogy with electrostatics can be drawn, and the nanoparticles can be considered as a homogeneous heat source distributed throughout the entire heated region [18]. Assuming that the bulk volume is thermalized, it is possible to rewrite equation 7 as a volume integral. The "thermal potential" integral for a cylindrical region of length $\ell$ and radius $w_0$, leads to [13]:

$$\Delta T_{\text{global}} = \frac{3}{2} \left( \frac{w_0 \ell}{a^2} \right) \left( \frac{C_{\text{m}}}{\rho_{\text{Au}}} \right) \Delta T_{\text{np}}. \tag{8}$$

Notice that, for colloids with a high mass concentration of gold nanoparticles, a significant global temperature rise is reached with considerable low local temperature increase at each particle [18].

In the present article, TL spectroscopy is explored to investigate the influence of NP size in photothermal heating probing gold nanospheres of different diameters. We experimentally demonstrate the correlation of $\text{J}_{\text{o}}$ and $\text{S}^2\text{F}$ with the increase in the temperature of the gold nanospheres, under continuous laser excitation.

# 2 Materials and methods

## 2.1 Materials

Gold nanospheres samples were selected to evaluate the collective heating of the colloid under CW laser irradiation. Citrate-stabilized colloidal samples of monodispersed Au nanosphere (less than 12% variability in size and shape), with diameter of 5 nm, 50 nm and 100 nm in deionized water were acquired from Sigma-Aldrich (Missouri, EUA). All samples were diluted in water, leading to colloids with the same gold mass (17.4 $\pm$ 1.2 mg/L).

## 2.2 Computational analysis

The absorption and scattering cross-sections of gold nanospheres were obtained using Mie Theory. The NP diameter was varied from 5 to 100 nm for spectroscopic analysis. The permittivity values of gold were obtained from Johnson & Christy reported results

[19]. To validate the computational procedure, its results were thoroughly evaluated by comparing them with spectroscopic results reported in the existing literature [20].

### 2.3 Thermal lens spectroscopy

The spatial ($r$) and temporal ($t$) temperature variation of the medium, taking into account the aberrant nature of the TL [21, 22], is given by:

$$\Delta T(r,t,\lambda) = \frac{2P\alpha_{\text{eff}}(\lambda)}{\pi C_{\text{p}}\rho w_0^2}\int_0^t \frac{1}{1+2t'/t_{\text{c}}}\exp\left(-\frac{2r^2/w_0^2}{1+2t'/t_{\text{c}}}\right)dt', \tag{9}$$

where $P$ is the laser power, $C_{\text{p}}$ and $\rho$ are respectively the heat capacity and the density of the medium, $w_0$ is the laser beam waist, $t_{\text{c}} = C_{\text{p}}\rho w_0^2/4\kappa_{\text{m}}$ is the characteristic buildup time constant, $\alpha_{\text{eff}}(\lambda) = \left[1-e^{-\alpha_{\text{a}}(\lambda)\ell}\right]/\ell$ defines an effective absorption coefficient taking into account the absorption coefficient ($\alpha_{\text{a}}$), and $\ell$ is the sample length. The temperature change induces a variation of the medium refraction index profile, generating a transient thermal lens.

The main characteristics of the measurement method are detailed in [23] where it has been extended the experimental procedure for weak absorption ($\alpha_{\text{a}}\ell \ll 1$) to higher-moderate ones ($\alpha_{\text{a}}\ell \leqslant 1$). The experimental measurement system integrates a Z-scan setup, where the sample moves along the propagation z-axis of the modulated laser beam, with a TL detection mode. In short, the setup explores a chopped 532 nm laser (Oxxius, LCX-532S) and a photodiode connected to a digital storage oscilloscope. The colloid was contained in a 1 cm cuvette placed at a translational stage.

The measured signal (S) is defined as the far field intensity change, with cell located at $z$. Considering the stationary regime (at t$\rightarrow\infty$), $S$ is given by:

$$S(\lambda) = -1 + \frac{1}{1-\left[\frac{P\ell(dn/dT)}{\lambda\ \kappa_{\text{m}}}\right]\alpha_{\text{eff}}(\lambda)\ \tan^{-1}\left(\frac{2V}{3+V^2}\right)}, \tag{10}$$

where $dn/dT$ is the thermo-optical coefficient of the medium, $V = z/z_{\text{R}}$, with $z_{\text{R}}$ being the Rayleigh distance ($z_{\text{R}} = \pi w_{0\text{f}}^2\,/\,\lambda$) and $w_{0\text{f}}$ is the focused beam-waist. Fitting the equation 10 to the normalized experimental data allows to obtain the $\alpha_{\text{eff}}$ value. The temperature distribution at the stationary regime is than obtained using equation 9. For further information , please refer to reference [24].

## 3 Results and discussions

Gold nanospheres with different sizes are well explored as nanoheaters for thermal applications. The optical properties of spherical gold nanoparticles are reliant on their size. Gold nanoparticles with small dimensions primarily absorb light with plasmonic peaks around the wavelength of 524 nm, whereas larger nanoparticles demonstrate increased light scattering and have peaks that broaden considerably and shift towards longer wavelengths. Moreover, with the increase in the diameter of a nanosphere, its absorption and scattering cross-section rise.

Equations 1 and 4, indicate the $\text{J}_{\text{o}}$ and $\text{S}^2\text{F}$ size dependence for a single nanoparticle. Figure 1 depicts the $\text{J}_{\text{o}}$ and $\text{S}^2\text{F}$ values for gold nanospheres with different

sizes (diameter), considering their maximum absorption cross-section at the plasmonic peak, in water. According to Figure 1, when exposed to short pulse illumination, smaller particles are better suited for attaining higher temperatures compared to larger structures (blue line). The $J_o$ values of the nanospheres with diameters of 5 nm and 50 nm are approximately four times higher than those of the 100 nm nanoparticles. Differently, under CW illumination, the $S^2F$ values (red line) indicate that single particles with large sizes can reach higher temperatures than smaller nanospheres when considered for single particle heating. In that case, the 100 nm (diameter) gold nanosphere shows a higher $S^2F$ value than 5 nm and 50 nm NP.

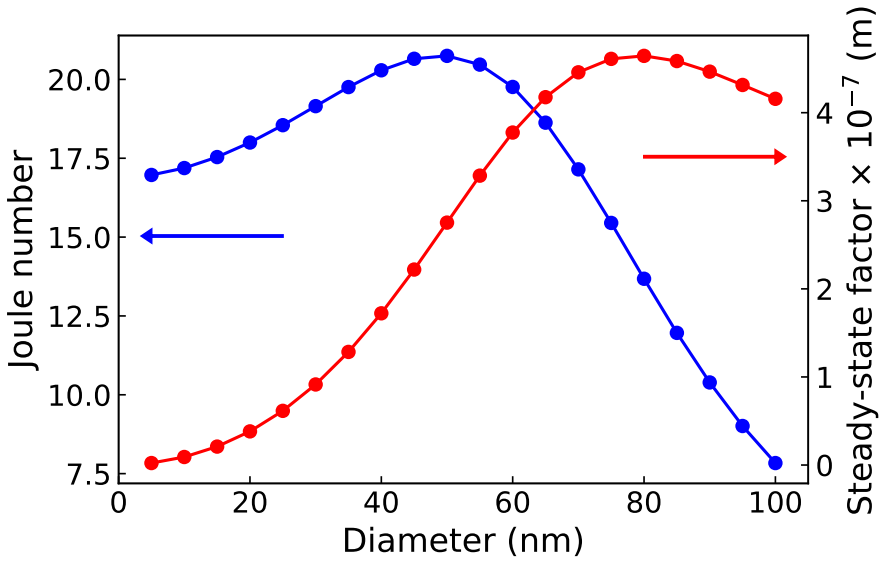


**Fig. 1** Gold nanosphere $J_o$ (blue) and $S^2F$ (red) values, as function of the NP diameter, obtained by Mie theory (in water).

On considering plasmonic colloidal volumes illuminated by laser, the absorbed light energy is proportional to the absorption coefficient of the suspension, which is given by: $\alpha_{abs} = C_m \sigma_{abs}/(\rho_{Au} V_{np})$. Figure 2 display the calculated absorption coefficient values of colloids, considering suspensions with different gold spheres diameters and same gold mass concentration (17.4 mg/L). Figure 2 indicates that $\alpha_{abs}$ values have similar behavior observed for $J_o$ (Figure 1, blue line), which indicates high values for gold nanospheres with 50 nm diameter. Therefore, the Joule Numbers turns to be an adequate Figure of Merit to identify colloidal nanoparticle size for efficient light absorption, independent of the illumination condition (pulsed or CW) of the plasmonic ensemble.

The photoheating of a nanoparticle ensemble can be described involving two distinct processes. First, the temperature of the nanoparticles increases, reaching an

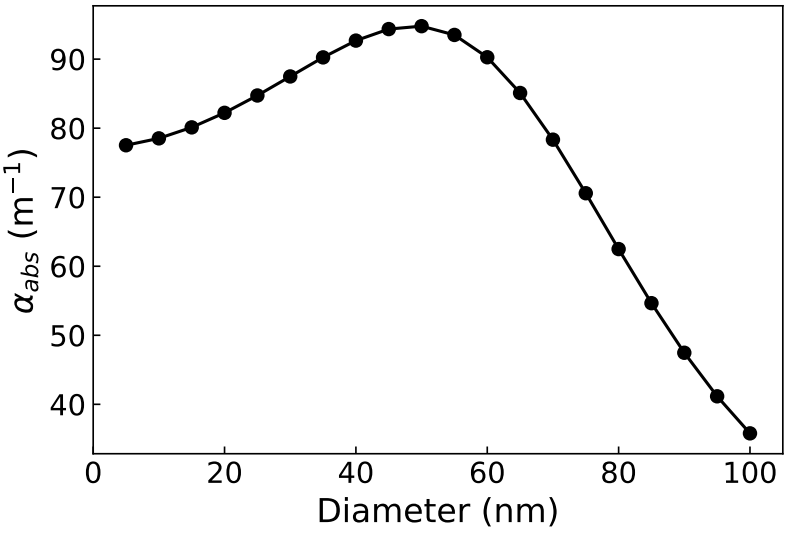


**Fig. 2** Calculated absorption coefficient of gold colloid nanospheres, with constant concentration of gold mass (17.4 mg/L).

intermediate steady state, with temperature ($\Delta T_{\rm np}$) given by equation 3. The intermediate steady-state temperature is the maximum temperature that a single (isolated) nanoparticle can achieve under CW illumination (or low repetition rate microsecond pulses). After, when the thermal fields from neighboring nanoparticles reach the surface of the nanosphere, the nanostructure temperature starts to increase again. This superposition effect leads to a global temperature ($\Delta T_{\rm global}$), described by Equation 7.

By using the TL technique, it is possible to infer the spatial temperature profile within a volume that has been subjected to laser heating. Figure 3(a) illustrates the time-dependent TL signal obtained from colloidal samples containing 50 nm diameter nanospheres, located at $V = 1.58$, when exposed to a laser power of 1.33 mW. The TL signals depicted in Figure 3(a) exhibit a characteristic buildup time ($t_{\rm c}$) of approximately 9.6 ms. The inset of Figure 3(a) shows the behavior of the $S$ versus V for the 50 nm gold nanospheres in water. The inset solid red line is the fitting of equation 10, which leads to $\alpha_{\rm a} = 92.2$ m $^{-1}$.

By analyzing the time-dependent TL signal, it is possible to uncover the sample temperature profiles. The global temperature distribution, shown in Figure 3(b) was attained after 44 ms (steady-state) of laser excitation time. The colloidal samples containing 50 nm and 5 nm NPs reached higher temperatures (up to $\sim 0.033$ m$^{\rm o}$C) compared to the one containing larger nanospheres, resembling the $J_{\rm o}$ behavior, shown in Figure 1 (blue line). This indicates that $J_{\rm o}$ is a suitable figure of merit for selecting high performance nanospheres for collective heating. As shown in Figure 3(b), the temperature increase in the colloidal sample containing 50 nm NPs is slightly greater than that achieved in the 5 nm NPs suspension. However, the obtained results are

subject to experimental error ($\sim 10\%$). Therefore, these two temperature profiles are considered statistically indistinguishable.

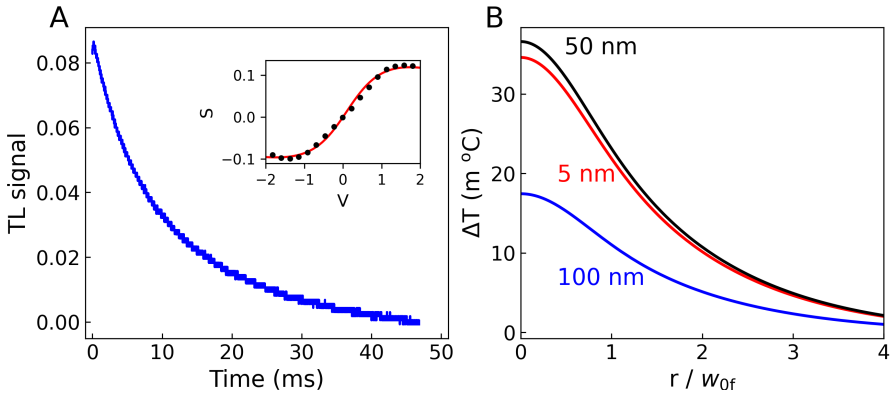


**Fig. 3** (a) Time behavior of TL signal of 50 nm colloidal Au nanospheres, at $V = 1.58$. The inset is far field intensity signal $S$ for distinct $V$ values. (b) Temperature change distribution of colloidal samples of Au nanospheres with different diameters (5, 50 and 100 nm), with $P = 1.33$ mW.

The global temperature of the illuminated sample is established by the thermal contribution of all nanoparticles (equation 7). Measuring $\Delta T_{\text{global}}$, the intermediate steady-state temperature could also be revealed, as described by equation 8. The obtained $\Delta T_{\text{np}}$ values are displayed in figure 4. Considering colloids with same gold mass concentration illuminated with 1.33 mW laser power, one can observe in figure 4(a) that the highest $\Delta T_{\text{np}}$ values are achieved on larger particles. Moreover, this result resembles the $S^2F$ behavior, as shown in figure 4(a), which simultaneously display the measured $\Delta T_{\text{np}}$ and calculated $S^2F$ values for different particle sizes. To the best of our knowledge, this is the first experimental study demonstrating that $S^2F$ is an appropriate figure of merit to identify high-performance plasmonic structures for (intermediate steady-state or single particle) optical heating. The $S^2F$-based selection of the plasmonic nanoheater can benefit applications that rely on the increase of the single particle temperature, as: bubble formation [25], plasmonic trapping and particle manipulation [26, 27].

The intermediate steady-state temperature of a single nanostructure enhances as the excitation laser power (or intensity) increases, as described by equation 3. Figure 4(b) depicts the reached $\Delta T_{\text{np}}$ values for different excitation powers, considering nanospheres with distinct sizes. Higher laser power leads to higher temperatures, maintaining the size-related behavior.

# 4 Conclusion

Theoretical analysis and thermal lens technique allowed us to identify micro-degree temperature changes of laser heated colloidal gold nanospheres of varying sizes. Our

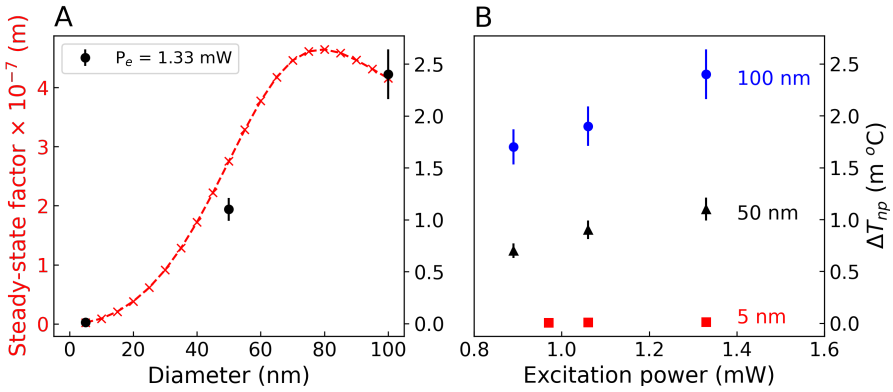


**Fig. 4** (a) Experimental (black) and theoretical (red) $S^2F$ values and intermediate steady-state temperature of a single nanostructure as function of NP diameter (illuminated with 1.33 mW laser power); (b) Experimental intermediate steady-state values for different excitation powers, considering 5, 50 and 100 nm diameter nanospheres.

measurements shows that the achieved TL global temperature resembles $J_o$ behavior. The optimal gold nanospheres diameter for efficient colloidal laser heating was identified to be 50 nm. The TL technique also enables the estimation of intermediate steady-state temperature of a single particle, which was shown to resemble $S^2F$ behavior. Such result leads to the understanding that single particle temperature is higher for bigger nanoparticle sizes, i.e., gold nanospheres with diameter larger than 80 nm. In this sense, the rules of using figures of merit to select efficient plasmonic nanoheaters were revealed and size dependence of plasmonic nanoparticle optical heating was disclosed.

# Declarations

**Author Contribution.** Conceptualization, R.E.A.; methodology, R.E.A.; validation, T.L.P.; formal analysis, T.L.P. and G.B.; investigation, G.B.; data curation, T.L.P.; supervision, R.E.A.; writing—original draft preparation, R.E.A., G.B. and T.L.P.; writing—review, R.E.A. and G.B. All authors have read and agreed to the published version of the manuscript.

**Funding.** This research was funded by Fundação de Amparo a Ciência e Tecnologia do Estado de Pernambuco - Brazil (FACEPE) and Conselho Nacional de Desenvolvimento Científico e Tecnológico - Brazil (CNPq). R. E. de A. and G. B. would like to acknowledge the financial support from the University of Angers, through the MIR project EPTON n°: E3617R60.

**Data Availability:.** The data that support the findings of this study are available on request from the corresponding author, upon reasonable request.

**Conflict of Interest.** The authors declare no competing interests.

# References


[1] Chen, M., He, Y., Hu, Y., Zhu, J.: Local heating control of plasmonic nanoparticles for different incident lights and nanoparticles. Plasmonics **14**(6), 1893–1902 (2019) https://doi.org/10.1007/s11468-019-00990-1

[2] Mehrzad, H., Habibimoghaddam, F., Mohajerani, E., Mohammadimasoudi, M.: Accurate quantification of photothermal heat originating from a plasmonic metasurface. Optics Letters **45**(8), 2355 (2020) https://doi.org/10.1364/ol.387789

[3] Cunha, J., Guo, T.-L., Alabastri, A., Zaccaria, R.P.: Tuning temperature gradients in subwavelength plasmonic nanocones with tilted illumination. Optics Letters **45**(19), 5472 (2020) https://doi.org/10.1364/ol.404950

[4] Borah, R., Kumar, A., Samantaray, M., Desai, A., Tseng, F.-G.: Photothermal heating of au nanorods and nanospheres: Temperature characteristics and strength of convective forces. Plasmonics **18**(4), 1449–1465 (2023) https://doi.org/10.1007/s11468-023-01855-4

[5] Zhao, L., Zhang, X., Wang, X., Guan, X., Zhang, W., Ma, J.: Recent advances in selective photothermal therapy of tumor. Journal of Nanobiotechnology **19**(1) (2021) https://doi.org/10.1186/s12951-021-01080-3

[6] Baffou, G., Polleux, J., Rigneault, H., Monneret, S.: Super-heating and microbubble generation around plasmonic nanoparticles under cw illumination. The Journal of Physical Chemistry C **118**(9), 4890–4898 (2014) https://doi.org/10.1021/jp411519k

[7] Lalonde, B.S.-L., Boulais, É., Lebrun, J.-J., Meunier, M.: Visible and near infrared resonance plasmonic enhanced nanosecond laser optoporation of cancer cells. Biomedical Optics Express **4**(4), 490 (2013) https://doi.org/10.1364/boe.4.000490

[8] Patskovsky, S., Qi, M., Meunier, M.: Single point single-cell nanoparticle mediated pulsed laser optoporation. The Analyst **145**(2), 523–529 (2020) https://doi.org/10.1039/c9an01869g

[9] Mantri, Y., Jokerst, J.V.: Engineering plasmonic nanoparticles for enhanced photoacoustic imaging. ACS Nano **14**(8), 9408–9422 (2020) https://doi.org/10.1021/acsnano.0c05215

[10] Yang, L., Yan, Z., Yang, L., Yang, J., Jin, M., Xing, X., Zhou, G., Shui, L.: Photothermal conversion of $SiO_2$@Au nanoparticles mediated by surface morphology of gold cluster layer. RSC Advances **10**(55), 33119–33128 (2020) https://doi.org/10.1039/d0ra06278b

[11] Chernov, G., Ibarra-Valdez, J.L., Carrillo-Torres, R.C., Medrano-Pesqueira, T.C.,

Chernov, V., Barboza-Flores, M.: Improved method of study on the photothermal effect of plasmonic nanoparticles by dynamic IR thermography. Plasmonics **14**(4), 935–944 (2018) https://doi.org/10.1007/s11468-018-0877-1

[12] L. Pedrosa, T., Farooq, S., Araujo, R.E.: Selecting high-performance gold nanorods for photothermal conversion. Nanomaterials **12**(23), 4188 (2022) https://doi.org/10.3390/nano12234188

[13] Pedrosa, T.L., Estupiñán-López, C., Araujo, R.E.: Temperature evaluation of colloidal nanoparticles by the thermal lens technique. Optics Express **28**(21), 31457 (2020) https://doi.org/10.1364/oe.405172

[14] Cruz, R.A., Marcano, A., Jacinto, C., Catunda, T.: Ultrasensitive thermal lens spectroscopy of water. Optics Letters **34**(12), 1882 (2009) https://doi.org/10.1364/ol.34.001882

[15] Lalisse, A., Tessier, G., Plain, J., Baffou, G.: Quantifying the efficiency of plasmonic materials for near-field enhancement and photothermal conversion. The Journal of Physical Chemistry C **119**(45), 25518–25528 (2015) https://doi.org/10.1021/acs.jpcc.5b09294

[16] Pitsillides, C.M., Joe, E.K., Wei, X., Anderson, R.R., Lin, C.P.: Selective cell targeting with light-absorbing microparticles and nanoparticles. Biophysical Journal **84**(6), 4023–4032 (2003) https://doi.org/10.1016/s0006-3495(03)75128-5

[17] Govorov, A.O., Zhang, W., Skeini, T., Richardson, H., Lee, J., Kotov, N.A.: Gold nanoparticle ensembles as heaters and actuators: melting and collective plasmon resonances. Nanoscale Research Letters **1**(1) (2006) https://doi.org/10.1007/s11671-006-9015-7

[18] Keblinski, P., Cahill, D.G., Bodapati, A., Sullivan, C.R., Taton, T.A.: Limits of localized heating by electromagnetically excited nanoparticles. Journal of Applied Physics **100**(5), 054305 (2006) https://doi.org/10.1063/1.2335783

[19] Johnson, P.B., Christy, R.W.: Optical constants of the noble metals. Physical Review B **6**(12), 4370–4379 (1972) https://doi.org/10.1103/physrevb.6.4370

[20] Haiss, W., Thanh, N.T.K., Aveyard, J., Fernig, D.G.: Determination of size and concentration of gold nanoparticles from UV-vis spectra. Analytical Chemistry **79**(11), 4215–4221 (2007) https://doi.org/10.1021/ac0702084

[21] Sheldon, S.J., Knight, L.V., Thorne, J.M.: Laser-induced thermal lens effect: a new theoretical model. Applied Optics **21**(9), 1663 (1982) https://doi.org/10.1364/ao.21.001663

[22] Carter, C.A., Harris, J.M.: Comparison of models describing the thermal lens effect. Applied Optics **23**(3), 476 (1984) https://doi.org/10.1364/ao.23.000476

[23] Zinoune, J.-B., Cassagne, C., Werts, M.H.V., Loumaigne, M., Chis, M., Boudebs, G.: Wavelength-dependence of the photothermal efficiency of gold nanoparticles in solution by z-scan photothermal lens spectroscopy. Chemical Physics Letters **823**, 140501 (2023) https://doi.org/10.1016/j.cplett.2023.140501

[24] Cassagne, C., Ba, O., Boudebs, G.: Time-resolved cw thermal z-scan for nanoparticles scattering evaluation in liquid suspension. Materials **15**(14), 5008 (2022) https://doi.org/10.3390/ma15145008

[25] Setoura, K., Ito, S., Miyasaka, H.: Stationary bubble formation and marangoni convection induced by CW laser heating of a single gold nanoparticle. Nanoscale **9**(2), 719–730 (2017) https://doi.org/10.1039/c6nr07990c

[26] Kotnala, A., Zheng, Y.: Opto-thermophoretic fiber tweezers. Nanophotonics **8**(3), 475–485 (2019) https://doi.org/10.1515/nanoph-2018-0226

[27] Samadi, M., Alibeigloo, P., Aqhili, A., Khosravi, M.A., Saeidi, F., Vasini, S., Ghorbanzadeh, M., Darbari, S., Moravvej-Farshi, M.K.: Plasmonic tweezers: Towards nanoscale manipulation. Optics and Lasers in Engineering **154**, 107001 (2022) https://doi.org/10.1016/j.optlaseng.2022.107001